ZCS and ZVS Power Converter Topologies for Variable Reluctance Machine Drives

Laurinda L.N. Reis, Leví P.B. de Oliveira, Edison R. da Silva, and Antonio M. N. Lima
Department of Electrical Engineering, Federal University of Paraiba
C.P. 10.105, Campina Grande, PB., 58.109-970 Brazil
Tel.: +55 (83) 310-1407, Fax: +55 (83) 310-1418, e-mail: edison@dee.ufpb.br

***Abstract* - This paper introduces a new soft-switched converter for variable reluctance motor drives. A DC voltage regulation is accomplished by a front-end switch that operates under zero-voltage-switching (ZVS) and also allows the current in the machine phase windings to commutate in a soft-switched mode. A DC-link controlled configuration operating under ZCS is employed as the basis for a comparative analysis. Different possibilities of control are analyzed. Simulated results confirm the feasibility of application of the proposed soft-switched technique to a SRM.**

I. Introduction

Switched Reluctance Motors (SRM) have simple and rugged construction. Successful applications of SRM drives have been reported from the fractional horsepower to several hundred kilowatts. For this reason many converter topologies for SRM drives have been proposed [1]-[3]. The Hard- Switched (HS) principles of the "classic", or asymmetric converter, and the DC link controlled configuration are presented in Fig. 1, for one phase. HS type, however, may cause high electro-magnetic interference (EMI) and lead to high switching losses. The soft-switching seems to cause less EMI and a number of techniques has been adapted to different topologies [4]-[6]. Among them, the DC-Link Controlled (DCLC) configuration presented in [4] has a reduced number of switches but operates with Pulse Density Modulation. Very recently, two new DCLC topologies that operate under ZCS and PWM control have been introduced [7]. Differently, the soft-switched "classic" converter has a greater number of switches but has the independent control of each of the motor phases and the relatively low voltage rating of the inverter components [5].

On the other hand, the primary disadvantage of an SRM is the higher torque ripple when compared to conventional machines, which contributes to acoustic noise and vibration. It is possible to reduce such ripple by electronic control [8].

This paper reviews the ZCS-DCLC configuration introduced in [7] for the purpose of comparison with a new soft-switched version of the classic configuration operating under ZVS. As a result different possibilities of control are analyzed. Simulated results confirm the feasibility of the proposed soft-switched SRM.

II. Basic DC-Link Controlled and Classic Configurations

The basic modes of operation of the DC-Link Controlled (DCLC) and the classic configurations can be understood from the schematic circuits presented in Fig. 1.

Mode I (powering mode): The DC link controlled configuration is in this mode when the switch K is in position M, and the switch S_W is on, so that $E_d = V_d$. For the classic configuration switches S_1 and S_2 are on and in both topologies the voltage V_d is directly applied across the phase. The correspondent phase current increases from either a null value or a minimum positive value on dependence of control.

Mode II (recovery mode): For the DC link controlled configuration, this mode is accomplished with switch K in position N and switch S_W turned-on, so that $E_d = -V_d$. For the classic configuration, switches S_1 and S_2 are off and the motor winding current flows through the diodes D_1 and D_2. Because a voltage - V_d is applied across that winding, its current decreases.

Mode III (freewheeling mode): In Mode III, for the DC link controlled configuration, either K is in position O and S_W is on or S_W is off. In both cases, $E_d = 0$ and the winding current freewheels by either S_W or D_o. For the classic configuration, this occurs with S_1 on (off) and S_2 off (on) causing the current to flow through S_1 (S_2) and D_1 (D_2).

III. Review of the ZCS DC-Link Controlled Converter

The basic power circuit of the proposed the DC link controlled configuration with single-phase input, is shown in Fig. 2. T_a, T_b, and T_c are used as the main switches that control the current through the motor windings. The symbol

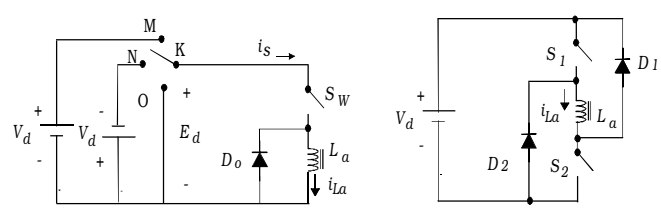

(a) DC link controlled configuration (b) Classic configuration

Fig. 1. Basic principles.

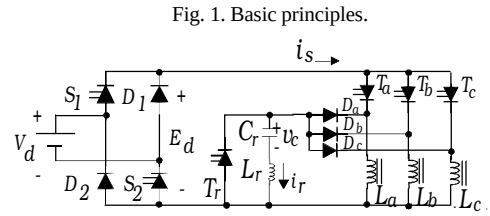

Fig. 2. First ZCS soft-switched converter.

used for these switches and switches S_1, S_2, and T_r indicates that they are controlled at turn-on and turn-off. The auxiliary commutation circuit consisting of the resonant inductor L_r, the resonant capacitor C_r, the auxiliary switch T_r, and the diodes D_a, D_b, and D_c allows to control the winding currents. The resonant circuit L_r-C_r enables zero current switching of the main switches. The auxiliary switch T_r reverses the capacitor voltage so that its polarity is adequate to commutate the main switch. D_a, D_b, and D_c avoid the circulation of current from the main switch to the auxiliary commutation circuit. The switches S_1, S_2, D_1, and D_2 are used for application of either positive or negative voltage to motor windings or to provide free-wheeling paths. Note that although switches with turn-on and turn-off control are indicated in the circuit, unidirectional and naturally commutated switches can be employed [7].

The simplified circuit for phase *a* is shown in Fig. 3. In this figure, S_W is the equivalent to S_1, S_2, and S_a in series for Mode I. For Mode II, $S_W = T_a$ and for Mode III S_W is the equivalent to S_1 (or S_2) in series with T_a. The transfer from one mode to another is accomplished with the help of the auxiliary commutation circuit.

Suppose the converter is operating in the powering mode for phase *a*. Therefore, T_a, S_1, and S_2 are conduction and T_r is off. Consider that the capacitor has been previously charged with an initial voltage $-V_c$ and that $|V_c| > |V_d|$. Figure 4 shows the operating stages for this case, which are explained next.

The commutation process starts when the switch T_r is fired [Stage I, reversing sub-mode in Fig. 4(a)]. As a consequence, the polarity of the capacitor voltage is reversed in a resonant way. Switch T_r turns off under ZCS. Then diode D_a conducts and the current in C_r, i_r, starts increasing in the reverse sense [Stage II in Fig. 4(b)]. When i_r equals the winding current, i_a, the current in T_a, i_s, becomes zero causing the main switch to be naturally commutated. In Stage III (discharging sub-mode) current i_a flows through D_a, L_r and C_r, charging linearly C_r with the initial polarity. Its limit is the point in which it stores enough energy for the next commutation. Such energy will guarantee that the current in the main switch of the same or another phase will become null in the stage II of the next switching cycle. This limit is practically controlled in terms of the voltage $v_{sw,}$ applied across switch S_w (representative of S_1, L_r, and T_a in series). When v_{sw} reaches the threshold value V_{swt}, $S_{a,}$ is fired. Depending on the control strategy either one of the switches of the front-end rectifier or none is turned on simultaneously with T_a. The current in $T_{a,}$ increases resonantly until the current in the diode becomes null (Stage IV).

Note that although these stages have been described for Mode I they can also occur in both modes II and III.

A 3-phase input version of this converter has been also proposed in [7]. Such version allows the input power factor control and is also useful when the converter must have the capability for dynamic breaking or regenerative operation.

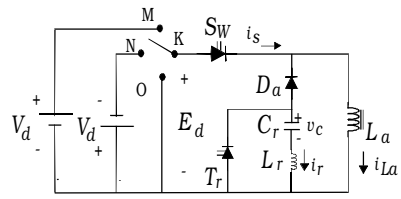

Fig. 3. Simplified circuit for the converter proposed.

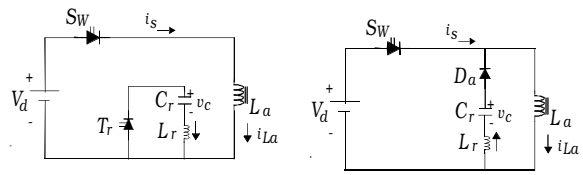

(a) Stage I: Reversing (b) Stage II: First resonant transition

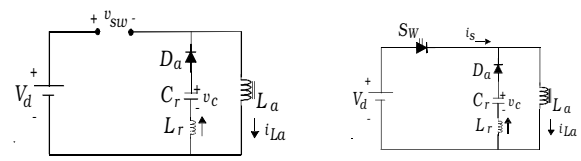

(c) Stage III: Discharging (d) Stage IV:Second resonant transition

Fig. 4. Sub-modes of operation that occur with any mode in Fig. 3.

IV. THE SOFT-SWITCHED 'CLASSIC' CONFIGURATION

The proposed soft-switched classic configuration in Fig. 5 operates under ZVS. It is based on the modified classic version presented in [5], which has the number of switches optimized for a number pair of phases. The auxiliary commutation circuit is similar to that presented in [12] but operates differently. The scheme is for an even number of phase-machines and IGBTs are explicitly shown. In this circuit the phase inductance, L_a for instance, is considered to be much greater than the resonant inductance L_r. Also, the capacitance of C_{r1} is greater than that of C_{r2}.

One cycle of operation is composed of eight stages (or sub-modes), as indicated in Fig. 6 (b) to 6(i) for the equivalent circuit of Fig. 6(a). They will be explained next with the help of the principal waveforms presented in Fig. 7.

Stage I (Freewheeling sub-mode, $t < t_1$): Suppose that initiallly the current in phase *a* is freewheeling through switch S_{ab}, diode D_a, and winding L_a, as shown in Fig. 6(b). Therefore, the current in phase *a* is decreasing. Suppose, also, that capacitor C_{r1} is charged with a negative voltage, $-V_d$, and C_{r2} is completely discharged. Switches S_m, S_r, and S_a are off during this interval.

Stage II (First resonant sub-mode, $t_1 < t < t_2$): In this stage, switches S_c, and S_a are turned-on under ZCS and ZVS, respectively. A resonant mode starts and the energy stored in capacitor C_{r1} is transfered to inductor L_r. This interval ends when the resonant current reaches the value I_a of the winding current i_{La} and diode D_a turns off.

Stage III (Second resonant sub-mode, $t_2 < t < t_3$): After D_{ab} stops conducting a new resonant mode starts charging

the capacitor C_{r2} with the help of the energy stored in L_r at the end of the previous interval, as shown in Fig. 6(d). This stage ends when the voltage in capacitor C_{r2} reaches the value V_d of the DC source and diode D_m turns on.

Stage IV (Third resonant sub-mode, $t_2 < t < t_3$): C_{r1} continues to charge resonantly until it reaches the value of the source voltage and D_0 starts conducting.

Stage V (Linear sub-mode, $t_4 < t < t_5$): During this interval, curent flows by either D_m or S_m. First, the excess of energy stored in the inductor is fed back to the source voltage V_d via the diode D_m. Next, D_m turns off and the current starts increasing in S_m while the current in L_a decreases, their sum being equal to the current in winding *a*. To guarantee ZVS turn on for S_m a gate signal is applied before D_m turn off.

Stage VI (Fourth resonant sub-mode, $t_5 < t < t_6$): A new oscillation starts, now through the path C_{r1}-L_r-D_m-S_r, until the capacitor voltage reverses completely.

Stage VII (Powering sub-mode, $t_6 < t < t_7$)**:** In this stage, the converter is in the powering sub-mode until the control commands turning off of S_m.

Stage VIII (Discharge of C_{r2}, $t_7 < t < t_8$); After S_m is turned-off under ZVS, the current in winding *a*, i_{La}, discharges C_{r2} and v_{Cr2} decreases linearly. When v_{Cr2} reaches zero, D_a starts conducting. This ends the operating cycle.

Employed together with the modes in Section II, these stages allows DC voltage regulation and current commutation in the phase windings.

V. Winding Current and Torque Control

The torque produced by SRM depends on the current and the self-inductance in each phase winding, that is,

$$T_{en} = \frac{1}{2}\frac{dL_n(\theta)}{d\theta} i_n^2 \quad (1)$$

where subscript *n* represents one of subscripts *a*, or *b*, or *c*, or *d*, or... for winding currents and inductances.

The total torque is given by

$$T_e = T_{ea} + T_{eb} + T_{ec} + T_{ed} + \ldots \quad (2)$$

The self-inductance varies according to the rotational angle θ of the motor. The characteristic of all the phases are approximately the same except that they are shift one in relation to the others.

The idealized motor inductance and winding current profiles are presented in Fig. 8(a) and Fig. 8(b). Current profiles can be realized using the following possibilities:

- The powering mode is applied for the winding current increase,
- A regulation is needed to limit the winding current, mainly at low speed,

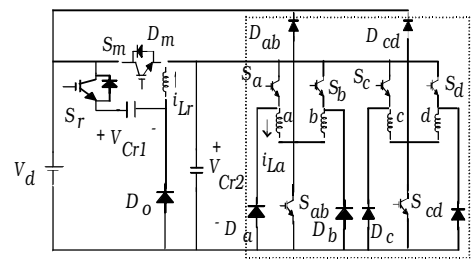

Fig. 5. Proposed ZVS converter.

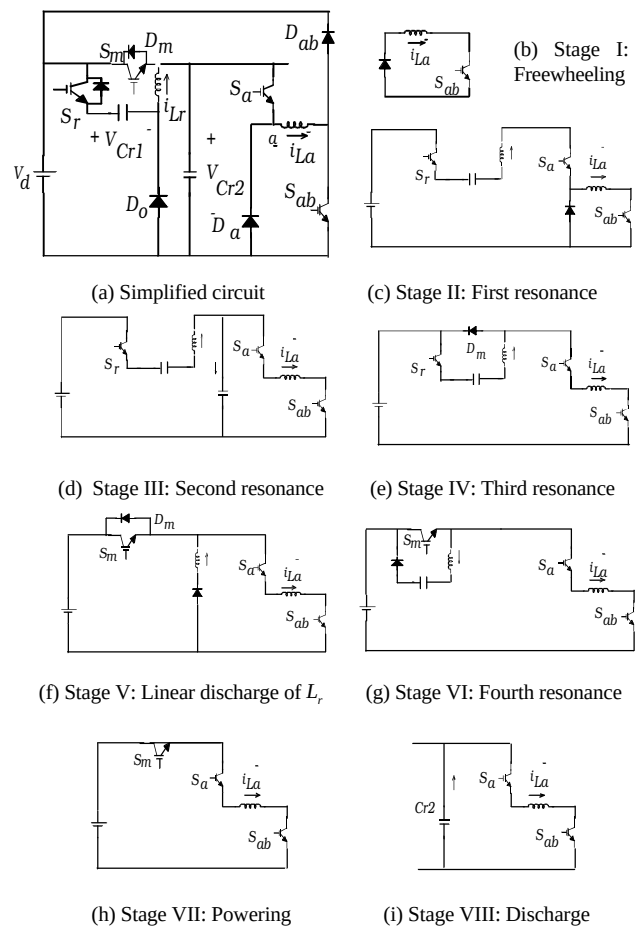

Fig. 6. Sub-modes of operation for the configuration in Fig. 5.

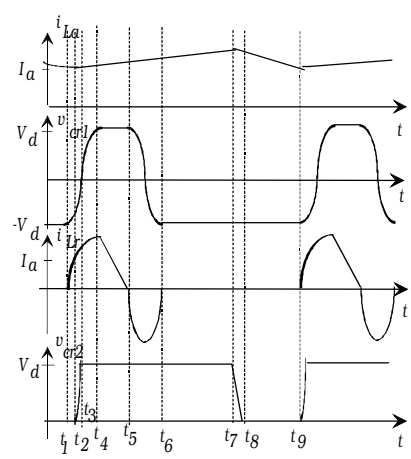

Fig. 7. Three methods for control of current with the ZCS converter.

- Either recovery or freewheeling mode or is applied to reduce the winding current towards zero,
- The current profile is shaped to improve the torque.

On the other hand, each inductance can be assumed to vary linearly up and down between a maximum and a minimum value, as schematically depicted in Fig. 9, in which β_s and β_r are parameters of the SRM and q is the number of phases [10]. The inductance can also be measured experimentally at different rotor positions. Since the inductance profiles are periodic in nature, in [8] they have been represented by a Fourier series with coefficients obtained by spectrum analysis from a 8/6 four-phase SR motor, that is

$$L_a = 0.000758 + .00047\cos\theta - .000071\cos 2\theta + 0.000009\cos 3\theta + .000032\cos 4\theta - .000022\cos 5\theta \quad (3)$$

Known the inductance and the current profiles, the torque can be calculated.

The different aspects mentioned above make different strategies to be possible. Some of them are discussed next.

A. Strategy I

Modes II and I alternate to regulate the phase current [Fig. 8(c)] by a "bang-bang" technique. For the DC-link controlled configuration T_a is turned off as in Fig. 4(a) and (b) each time the winding current reaches either a maximum or a minimum and then fired again to start Mode II or Mode I, respectively. Instead of Mode II, Mode III can be used as in Fig. 8(d). For the classic configuration, S_a and S_{ab} are turned off and turned on as necessary. At the moment desired, only Mode II is employed and the winding current is reduced to zero. It is also possible to use Modes I, II and II in sequence as Fig. 8(e) [7].

Anyone of the possibilities above produces discontinuities in the torque during transition causing a high torque ripple.

B. Overlapping Strategies.

It is possible to minimize such ripple during transition by overlapping phase currents. Some approaches allow the stator phase currents to be overlapped during the commutation interval.

B.1. Strategy II

Consider currents in phase *a* and phase *b*, as an example. This approach keeps phase *a* in its discharging stage until the phase current reduces to zero, while the converter is simultaneously operating in the powering mode for phase *b*. This is a mid term between applying reverse and freewheeling modes for decreasing the winding current. This strategy can be used as a variation of any of the previous methods replacing the final reversing mode.

The overlapping process between phases *a* and *b* can be understood from the simplified circuit in Fig. 10 for the DCLC configuration, in which overlapping is employed with the technique in Fig. 8(d). After operating in freewheeling

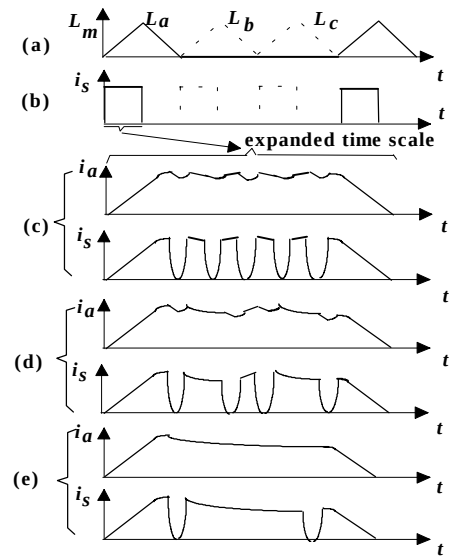

Fig. 8. Self-inductance and current profiles; methods for current control.

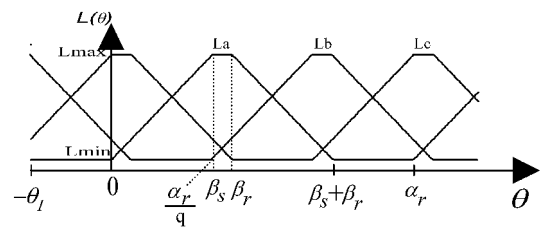

Fig. 9. Variable winding inductance in SRM of q phases

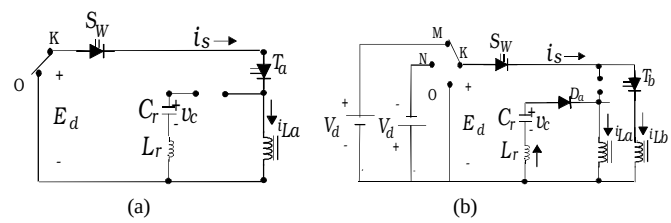

Fig.10. Illustrative stages for overlapping between phases A and B

[Fig. (a)], the topology is changed to the situation in Fig. 10(b), in which phase *b* is fed by voltage V_d while phase *a* discharges. In the case of the DCLC, the capacitor charges until the current in winding *a*, i_a, becomes null. Therefore, its voltage tends to large values and techniques to limit these values have been mentioned in [7]. The limitation caused by the fact that two phases can not simultaneously operate in different modes in that topology makes the control circuit to be complex. The classic configuration allows an easier implementation but the almost square current profiles, with null values in certain positions, cause high ripple in the torque. The increase in the number of phases tends to improve the torque.

B.2. Strategy III

The strategy here described was introduced in [8]. It consists of an improved PWM current control technique for torque ripple minimization in the low speed mode of operation With this purpose, the torque pulsations during commutation are minimized by simultaneous conduction of

two positive torque producing phases over an extended predefined region. The torque control strategy is based on following a contour for each of the phases of the SR motor such that the sum of torques produced by each phase is constant and equals the desired torque T^* In order to achieve this constant torque, a contour function $f_T(\theta)$ is defined such that

$$T_{total} = T^* f_T(\theta) \tag{4}$$

where

$$f_T(t)\sum_n f_n(\theta) = 1 \quad \text{for} \quad n = a, b, c, d, ..., q \tag{5}$$

where f_n is the contour function for each one of the q phases.

One possible choice for the contour function $f_T(\theta)$ for a four phase 8/6 SRM is shown in Fig. 11. The equation of the function for phase a is [8]

$$\begin{aligned} f_a &= .5 - .5\cos 4(\theta - \theta_o), && \text{for } \theta_o \le \theta \le \theta_1 \\ &= 1, && \text{for } \theta_1 \le \theta \le \theta_2 \\ f_a &= .5 + .5\cos 4(\theta - \theta_o) && \text{for } \theta_1 \le \theta \le \theta_3 \\ &= 0, && \text{otherwise.} \end{aligned} \tag{6}$$

The contour function is positive only during its positive inductance slope and the choice of the reference angles depends on the inductance profile of a particular motor.

The torque control strategy forces the outgoing phase current to follow a decaying contour rather than either forcing it to go to zero by application of reverse voltage or allowing it to freewheel naturally. The incoming phase is also forced to follow an increasing contour by active control. Four phase SRM's are readily adaptable to this scheme since there is a region in the inductance profiles of two adjacent phases where they simultaneously possess positive slopes.

The soft-switched classic configuration proposed is more flexible than the DCLC configuration for controlling the current profile. It should be noted that the current profile can also be achieved by varying the source voltage. In this configuration, freewheeling may occur by either paths S_{ab}-D_a or or S_{ab}-D_{ab}-S_m. Also, switch S_a can conduct at same time currents in phase a and phase b, independently of each one be in either powering, reverse or freewheeling mode.

VI. Simulated results

With the purpose of outlining the advantages of the proposed circuit, a simulation was performed with the DCCL configuration for a three phase SRM drive. For the circuit, the following parameters have been used: $V_d = 100$ V, $I_a^* = I_b^* = I_c^* = 5$ A, $C_r = 1$ μF, $L_r = 80$ μH and a variation of current of 0.5 A. For the motor, $\omega_m = 1900$ rpm, $L_{max} = 110$ mH, $L_{min} = 10$ mH, $\beta_s = 0.35$ $rad.$, $\beta_r = 0.42$ $rad.$, $\alpha_r = 1.05$ $rad.$ The winding resistance has been considered to be $R_s = 0.5$ Ω. Figure 12 shows the simulation results for the circuit in Fig. 2 operating with three phases ($q = 3$), Strategy I and the self-inductance as in Fig. 9. It should be

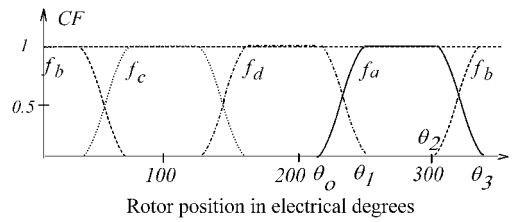

Fig. 11. Contour functions (CF) for profiling individual phase currents

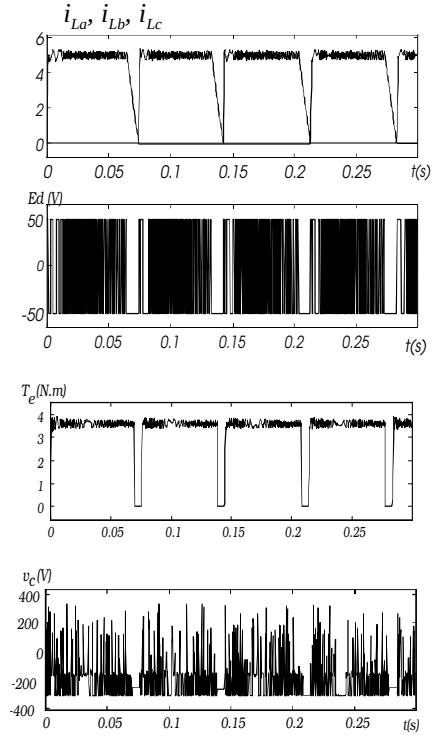

Fig. 12. Bus voltage, phase current, torque, and capacitor voltage for the circuit in Fig. 2: $q = 3$, without overlapping (Strategy I).

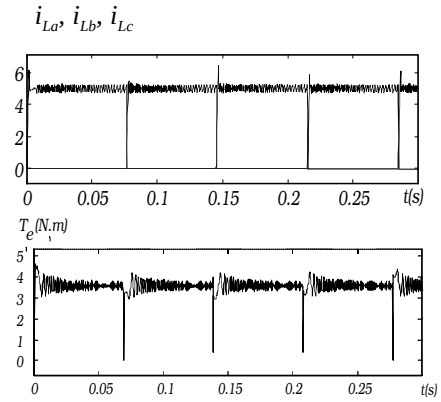

Fig. 13. C urrent in one of the phases and torque for the circuit in Fig. 2: $q = 3$ and overlapping (Strategy II)

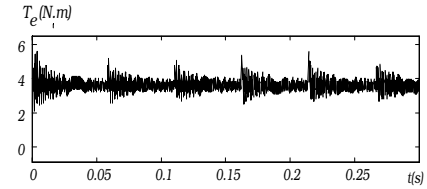

Fig. 14. Torque for the circuit in Fig. 2: $q = 4$ and overlapping (Strategy II)

noticed the ripple in the torque and the high peaks in the capacitor voltage. Figure 13 shows that Strategy II for overlapping improves the torque shape (Fig. 13) when compared to the case without overlapping of Fig. 12. With $q = 4$ the torque shape is additionally improved and eliminates discontinuities, as shown in Fig. 14.

Strategy III was used in the simulation of the configuration proposed in Fig. 5, in which $V_d = 50\ V$, $C_{r2} = 100\ nF$, $C_{r2} = 10\ nF$, $L_r = 3\ \mu H$. The converter was applied to a 8/6 four-phase SRM having a maximum inductance of *1.2 mH* and a minimum inductance of *0.26 mH* and a winding resistance of *0.3* Ω. The phase current was regulated to follow the contour of equation (6) by "bang-bang" control. The overall block diagram of the controller used with Strategy III for four phases is shown in Fig. 15 [8]. The actual current is sensed and fed back to the controller to generate the error after comparing with the reference current. The error is passed through a PI controller which generates the desired duty-cycle for the active phase or phases. An encoder is used to feedback the rotor position continuosly to the controller. The torque is regulated in the inner loop. The speed error signal generates the torque command which is the input to the controller. The T-I–θ characteristics have been obtained from the self-inductance data given in equation (3). The desired current determined this way is compared with the actual current, and the generated switching pattern is fed to the power converter.

The simulated results in Fig. 16 favors the use of the proposed configuration used with Strategy III, when compared to the DCLC configuration used with strategy II. It can be seen that the phase winding currents follow the imposed contour, the torque ripple is more regular and minimized and the voltage peaks in both capacitors are limited to the source value.

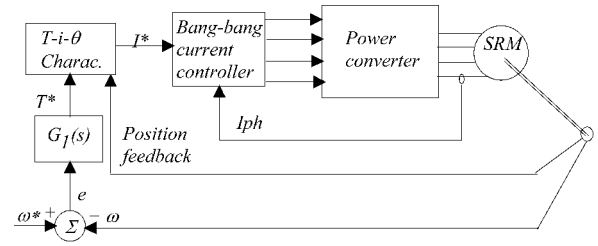

Fig. 15. Block diagram of the SRM drive with torque ripple minimization.

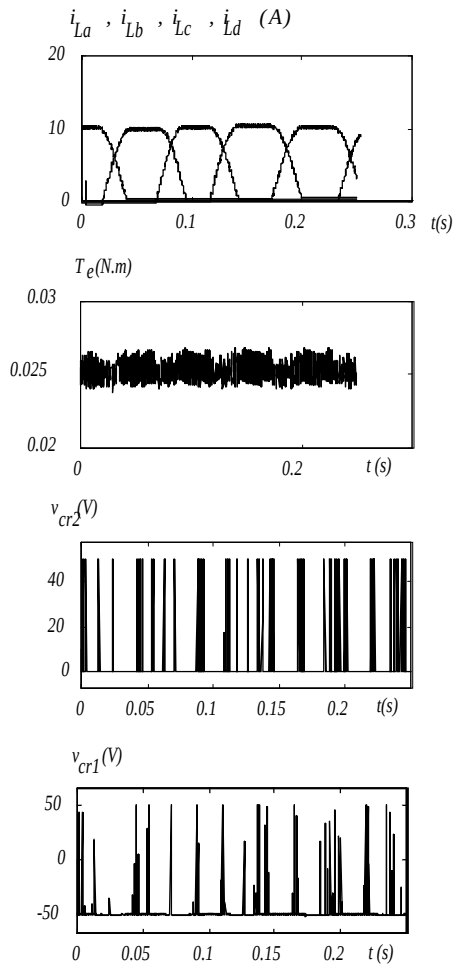

Fig. 16. Phase winding currents, torque, and capacitor voltages v_{Cr2} and v_{Cr1} for the circuit in Fig. 5: four phases with overlapping (Strategy III).

CONCLUSION

This paper has proposed a new ZVS topology for variable reluctance drives. Also a DC-link controlled (DCLC) configuration, operating under ZCS, has been reviewed for the purpose of comparison. The analysis of these topologies have been done through their equivalent circuit. Two different possibilities of control have been discussed in detail. Although the DCLC configuration has a reduced number of components and is able to eliminate torque discontinuities, these are accomplished at the expenses of either high peak voltages across the resonant capacitor or a more complex control. A more regular torque shape has been obtained with the proposed topology operating with a strategy of torque ripple minimization. It has also been shown that the voltage peaks in the existing capacitors are limited to the source value.

REFERENCES

[1] A. Hava, V. Blasko, and T.A. Lipo, "A modified C-dump converter for switched reluctance machines", IEEE IAS'91 Conference Record, 1991, pp. 886-891.

[2] S. Vukosavic and V. Stefanovic, "SRM inverter topologies: a comparative evaluation", *IEEE Trans. on Ind. Appl.*, Vol. 27, No. 6, Nov./Dec. 1991, pp. 1034-1047.

[3] M. Ehsani, J.T. Bass, T.J.E. Miller, and R.L. Steigerwald, "Development of a unipolar converter for switched reluctance motor drives", *IEEE Trans on Ind. Appl.*, vol. IA-23, No. 3, 1987, pp. 545-553.

[4] S.S. Park and T.A. Lipo, "New series resonant converter for variable reluctance motor drive", Research Report 92-9, WEMPEC, University of Wisconsin-Madison, March 1992.

[5] G.H. Rim, W.H. Kim, and J.G. Cho, "ZVT Single Pulse-Current Converter for Switched Reluctance Motor Drives", IEEE APEC'96 Conference Record, 1996, pp. 949-955.

[6] Y. Murai, J. Cheng, and M. Yoshida, "A soft-switched reluctance motor drive circuit with improved performances", IEEE PESC'97 Conference Record, 1997, pp. 881-886.